Intermittency of rheological regimes in uniform liquid-granular flows

Aronne Armanini,* Michele Larcher, and Luigi Fraccarollo
CUDAM, University of Trento, via Mesiano 77, I-38100 Trento, Italy
(Received 2 February 2009; published 22 May 2009)

We present a detailed analysis of a free surface-saturated liquid-granular mixture flowing over a static loose bed of grains, where the coexistence of layers dominated by collisional and frictional interactions among particles was observed. Kinetic theory was applied to the flow described above and it proved suitable for describing a realistic behavior of the collisional layers, although it failed to interpret the regions of the flow domain dominated by the frictional contacts. The paper provides a conceptual scheme with which to overcome this problem by focusing on the mechanisms governing the transition from the frictional to the collisional regime. In particular we observed that in highly concentrated flows the transition layer exhibits a typical intermittency of the dominating rheological regime, switching alternately from the frictional to the collisional one. By filtering the velocity signal, we introduced an intermittency function that made it possible to extend the validity of the equations derived from dense gas analogy, typical of the collisional regimes, also in the intermittent phase of the flow. Owing to the small values of the Stokes number, in the application of the kinetic theory we accounted for the possible variation of the elastic restitution coefficient along the flow depth.

DOI: 10.1103/PhysRevE.79.051306 PACS number(s): 45.70.Mg, 47.57.Gc, 05.20.Dd

I. INTRODUCTION

A granular material subjected to deformation may give rise to different types of interactions among grains and generate stresses through different mechanisms. Individual particles may interact with the others in form of clusters, generating a network of forces through sustained rolling or sliding contacts or by nearly instantaneous collisions, during which the energy is dissipated because of inelasticity and friction. The relative importance of these mechanisms may be used as the characteristics defining the various flow regimes [1]. Dense gas analogy has led to a great deal of work being done on the application of kinetic theories to granular materials, the intention being to derive a set of continuum equations entirely from microscopic models of individual particle interactions. These models are based on the assumption that particles interact by instantaneous binary collisions. The grains are modeled in a simple way, ignoring surface friction or any other particle interaction tangential to the contact point, and considering a constant coefficient of restitution to represent the energy dissipated by the impacts among the particles. The corresponding regime, often described as *collisional*, has been widely studied by many authors [2]. There is instead a *frictional regime* which is typical of slow, dense flows of granular materials, where the grains move with sustained contacts, to which the dense gas analogy cannot be applied [3].

The two regimes are often considered to occur separately. The Stokes number or the Bagnold number (ratios between collisional and frictional stress) [4–6] are needed to discriminate the two types of granular flow. Under the action of gravity the two regimes appear to be stratified, with the collisional one prevailing near the free surface and the frictional one near the bed.

In this paper we will show that the two regimes coexist to a large extent and that they interact intermittently. With an opportune filtering of the signal the equations derived from dense gas analogy for the collisional regimes are valid also during the intermittent phase of the flow.

II. DESCRIPTION OF THE EXPERIMENTS

In suitable experimental circumstances liquid-granular channel flows occur in equilibrium conditions, in the sense that a moving layer of particles flows over a static loose bed of water-saturated grains. In this case the bed represents an interface where the vertical profiles of the different quantities, such as velocity, concentration, and granular temperature, do not change abruptly or exhibit cusps, but tend asymptotically to the static values. This condition is remarkably different from those that develop over a solid bed [6]. With opportune conditions at the downstream end of the channel and under constant upstream feeding of water and particles, the deposit layer forms spontaneously and the flowing layer adjusts its depth through erosion or accretion of the static deposit.

Experiments were carried out in a special flume (6 m long and 0.1 m wide) at the Hydraulics Laboratory of the University of Trento. The channel can be tilted at angles ranging from 0° to 22°.

The flume was fitted with a weir at the end in order to create an upstream backwater effect and induce the formation of the deposited layer [5]. It is easy to show that, under constant upstream feeding of water and sediments, the flow upstream of the weir is uniform (Fig. 1).

During an experimental run, the setup formed a closed loop, in which a fixed volume of water and granular material circulated. Identical spherical plastic particles ($D=6.0$ mm) were selected as granular material with a specific gravity $\rho_p/\rho=2.21$, where ρ_p and ρ denote the densities of the granular material and of the interstitial fluid, respectively.

Liquid-granular flows were photographed through the transparent flume sidewall using a grayscale high-speed digital camera with a resolution of 1280×1024 pixels and a

*aronne.armanini@unitn.it

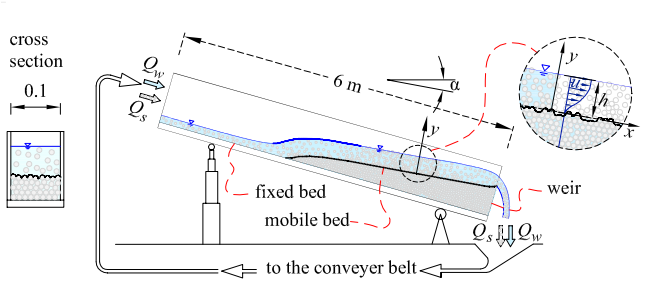

FIG. 1. (Color online) Sketch of the channel with the indication of the coordinate system [7].

frame rate up to 1000 fps. Imaging techniques were applied to a succession of a sufficiently long series of consecutive frames (approximately 3000). The methods were developed specifically to derive the local kinematics of each single particle seen through the sidewall and estimating the local concentration of the solid phase [8,9]. In this way a complete data set, consisting of more than 10^6 velocity and concentration data, was obtained for each run [10]. The near-wall volumetric concentration was measured using three-dimensional stereoscopic Voronoï imaging methods specifically developed to measure near-wall particulate flows of opaque particles observed through a transparent wall [9]. These methods are able to handle position and motion ambiguities, as well as particle occlusion effects, which are difficulties common in the case of dense dispersions of many identical particles. Considering the large number of data, the raw measurements could be processed also using low-level and high-level statistical tools in order to extract statistically meaningful estimates of the macroscopic and microstructural features of the flow. In particular for the purpose of the present paper, data could be used to characterize particle arrangements and to evaluate the mean and fluctuation velocities, the granular temperature, and the local concentration. Statistical tools based on the Lagrangian velocity autocorrelation function and on the Eulerian radial velocity correlation functions were employed to purge granular temperature estimates of the measurement noise. For further details on the technique used to correct the granular temperature and velocity, see [10,11]. The measurements proved to be affected only by relatively small errors and were suitable for the comparison to the application of kinetic theory.

III. INTERPRETATION OF THE RESULTS ACCORDING TO THE KINETIC THEORY

The application of kinetic theory to this uniform liquid-granular flow gives rise to the following formulation for the normal and the tangential stresses:

$$\sigma_c = (1 + 4cg_o)c\rho_p\Theta, \tag{1}$$

$$\tau_c = g_o f_2 \rho_p \Theta^{1/2} D \frac{du}{dy}, \tag{2}$$

where $g_o(c)$ represents the radial distribution function, for which we have adopted the form proposed by Lun and Savage [12]

$$g_o(c) = \frac{1}{(1 - c/c_*)^{2.5c_*}}, \tag{3}$$

where c is the particle concentration and c_* is its maximum value, which has been taken here to be 0.672. D is the diameter of particles and du/dy the shear rate (y is the coordinate normal to the bed). $\Theta = \langle \Sigma_{j=1}^{3} (u_j - \langle u_j \rangle)^2 \rangle / 3$ is the granular temperature, with u_j and $\langle u_j \rangle$ being the instantaneous and the average velocity components of the particles.

For the constitutive dimensionless function f_2 we have chosen the form proposed by Lun *et al.* [13] based on the theory of inelastic particles, and that depends also on the inelastic restitution coefficient because we have observed the importance to accounting for the reduction of the inelastic restitution coefficient due to the effect of the interstitial fluid. In this case

$$f_2 = \frac{5\sqrt{\pi}}{96\eta_p(2-\eta_p)}\left(1 + \frac{8}{5}\eta_p c g_o\right) + \left(\frac{1}{g_o}\frac{8}{5}\eta_p(3\eta_p - 2)c\right) + \frac{8}{5\sqrt{\pi}}\eta_p c^2 g_o, \tag{4}$$

with $\eta_p = (1+e)/2$.

The coefficient of restitution e has been observed to depend significantly on the Stokes number [4,14]. The Stokes number represents the ratio of two time scales: the particle response time, $(1/18)\rho_p D^2/\mu$, expressing the deceleration of the particle due to the viscous drag force $3\pi\mu DV$, and a characteristic time scale of the flow, typically assumed as the time D/V needed for a particle with the velocity V to move a distance of one diameter D through the liquid

$$\mathrm{St} = \frac{1}{18}\frac{\rho_p DV}{\mu}. \tag{5}$$

In the case of granular-liquid channel flows driven by gravity, the fluctuation velocity $\Theta^{0.5}$ can be chosen [5,6] as representative velocity in Eq. (5), leading to the following definition of the Stokes number:

$$\mathrm{St} = \frac{1}{18}\frac{\rho_p D\Theta^{0.5}}{\mu}. \tag{6}$$

However the relation between the restitution coefficient and the Stokes number was determined in a different experimental frame that required the adoption of a slightly different formulation. One spherical particle, identical to the ones used for the channel flow experiments, was released and then driven by gravity in a receptacle filled in each test with a fluid of different viscosity. The motion of the sphere was measured using a high-speed camera before, during, and after the collision with a rigid plate at the bottom of the receptacle [15]. In this condition the representative velocity can be set to $V = 2U$ [16] in Eq. (5), where U is the particle speed relative to the collision plate before the impact. This leads to the following formulation for the Stokes number: $(1/9)\rho_p UD/\mu$. The restitution coefficient depends significantly on the Stokes number, ranging from 0 for $\mathrm{St} \leq 10$ to 0.9 for $\mathrm{St} > \sim 10^4$. In the experiments reported here, the Stokes number was always $< \sim 200$ and the corresponding

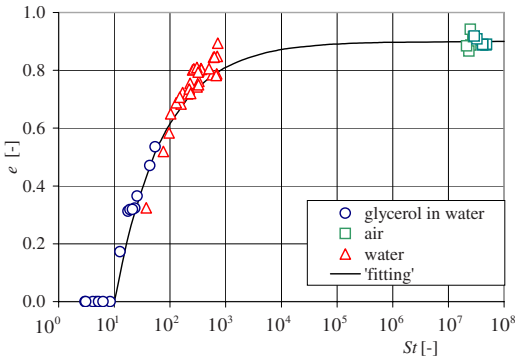

FIG. 2. (Color online) Behavior of restitution inelastic coefficient e_p as function of the Stokes number [15].

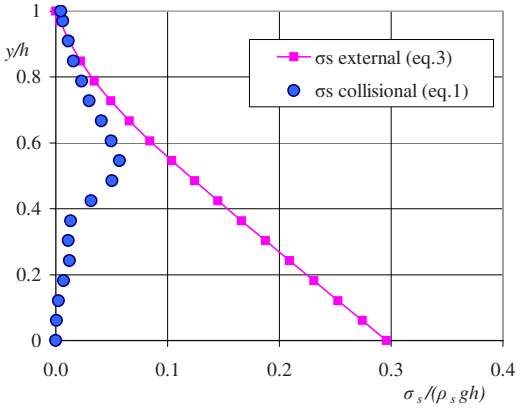

FIG. 3. (Color online) Experimental data: distribution of external and internal [collisional Eq. (1)] normal stresses; $h=62$ mm, $\alpha=8°$.

inelastic restitution coefficient was from 0 to 0.70. Figure 2 reports the experimental data, fitted by the following regression equation:

$$e = 0.9 - 2.85\mathrm{St}^{-0.5}. \tag{7}$$

The experimental results reported in Fig. 2 are in very close agreement with the findings of Joseph *et al.* [4] and of Gondret *et al.* [14].

If the flow is uniform, the shear stresses and the normal stresses among the particles are balanced by the corresponding components of the gravitational forces (external stresses)

$$\sigma_e = (\rho_p - \rho) g \bar{c} \cos \alpha (h - y), \tag{8}$$

$$\tau_e = g[\rho + \bar{c}(\rho_p - \rho)] \sin \alpha (h - y). \tag{9}$$

Here h is the flow depth measured in the normal direction, g the acceleration of gravity, α the slope angle of the flow, and $\bar{c}=(\int_y^h c dy)/(h-y)$ represents the concentration integrated over the normal distance $h-y$. In this case the tangential projection of the entire burden of the flow (water+grains) [Eq. (9)] is charged over the solid phase only [Eq. (2)] assuming that the shear stress in the liquid phase is negligibly small.

Armanini *et al.* [6] describe the presence of a stratification of rheological mechanisms across the flow depth, with the frictional regime located in the slower regions and the collisional layers where velocity and shear rate are greater. In fact, if the mixture is completely saturated, the external stresses [Eqs. (8) and (9)] are well balanced by the collisional internal stresses [Eqs. (1) and (2)] near to the free surface, while near to the erodible bed the comparison (Fig. 3) is completely unsatisfactory: here the external stresses have their maxima, while the collisional internal stresses tend to be suppressed.

IV. INTERMITTENCE BETWEEN COLLISIONAL AND FRICTIONAL REGIMES

The visual record of the motion of the particles near to the bed shows the dominance of nearly continuous sliding among the particles with prolonged contacts typical of the frictional regime (Fig. 4, particles marked with red crosses). In the experiments reported here we observed not only that a stratification of rheological mechanisms occurred but also that collisional and frictional regimes could coexist, in the sense that they alternated in time. This alternation of different regimes was similar to what happens on the border of a turbulent boundary layer where the alternation between turbulent flow and external potential flow is identified as the phenomenon of intermittency [17]. This picture of the flow domain was different than the observations keeping collisional and frictional mechanisms in distinct kinds of experiments.

In the case of granular flow the intermittency could be calculated by analyzing the time evolution of the vertical velocity of particles. In fact in the frictional regime, particles rolled in relatively ordered layers, one on top of the other, and the vertical velocity changed in time according to regular sequences, characterized by some peaks at regular intervals. Observation of the vertical velocity history shows that this component of the velocity can periodically exceed these peak values typical of the frictional regime, indicating that the rheological mechanism has switched to collisional conditions.

In order to define the intermittency, it is necessary to determine a threshold value for the velocity fluctuation below which the regime has to be considered purely frictional. Estimation of this threshold can be made by considering a spherical particle rolling along a line connecting the hollows of the surface composed by spheres of the same diameter with the centers lying on a plane. The fluctuating component of the vertical velocity is

$$u_y' = \left(\sqrt{3} - \sqrt{\frac{8}{3}}\right) D \frac{du_x}{dy}. \tag{10}$$

In this case two adjacent planes have a direction of displacement inclined at 60°; that is, in a average one-directional flow the particle zigzags also in the lateral direction. This is rather unrealistic. In the real case a particle rolling over the underneath layer is subject to wider oscillations. In fact the particles of the lower layer are not aligned on a plane and during the frictional motion each layer in turn is in motion and therefore the particles that make up the lower layer pos-

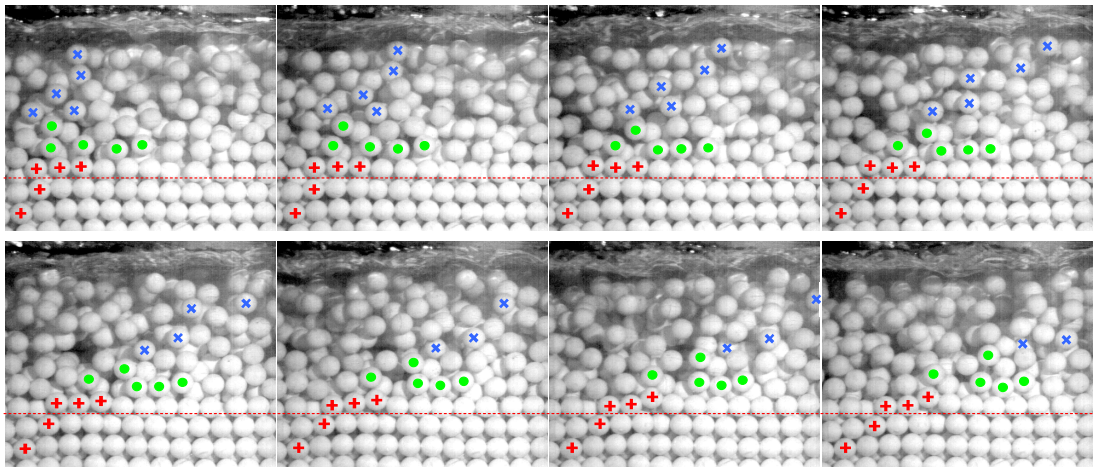

FIG. 4. (Color online) Sequence of images of a granular-liquid uniform flow over a mobile bed, acquired through the flume sidewall at a frame rate of 500 Hz (but presented here at 100 Hz). The flow spans from the frictional regime (bottom layers) to the fully developed collisional regime (top layers) through a transition zone characterized by the intermittence of the two regimes. In the images some particles are marked with colored symbols in order to highlight their displacements using red crosses for the frictional layers, a blue × for the collisional layers, and green bullets for the intermittence-dominated layers. A thin horizontal dashed line is inserted in the figure in order to show the vertical displacements of the particles in the frictional layers moving in form of an ordered stratification of particle chains.

sess their own vertical velocity. For this reason, one would expect the coefficient appearing in Eq. (10) to be remarkably higher. By fitting the experimental data in light of the procedure now described, the following expression has been adopted:

$$u_y' = 1.6D\frac{du_x}{dy}. \tag{11}$$

This threshold may seem to be too high for the particles in the layer completely dominated by the frictional forces (particles marked with red crosses in Fig. 4), but in this case the granular temperature is generally so small that even with a smaller threshold value the final result on the collisional part of the temperature does not appreciably change. By contrast, it is important to keep the threshold value sufficiently high in the layer dominated by the intermittency, as is evident in the sequence reported in Fig. 4 for the particles labeled with green bullets. In this case the coefficient in Eq. (10) could reasonably be of the order of unity.

An example of the decomposition of the velocity signal following the definition of the intermittence factor is shown in Fig. 5. In particular, panel a) shows a specimen of the time record of the vertical nondimensional fluctuating velocity of the particles, while panels b) and c) restrict the representation to the collisional and frictional sequences, respectively. The measurements are taken at a position $y/h=0.62$. The dashed red lines represent the threshold value of the fluctuating com-

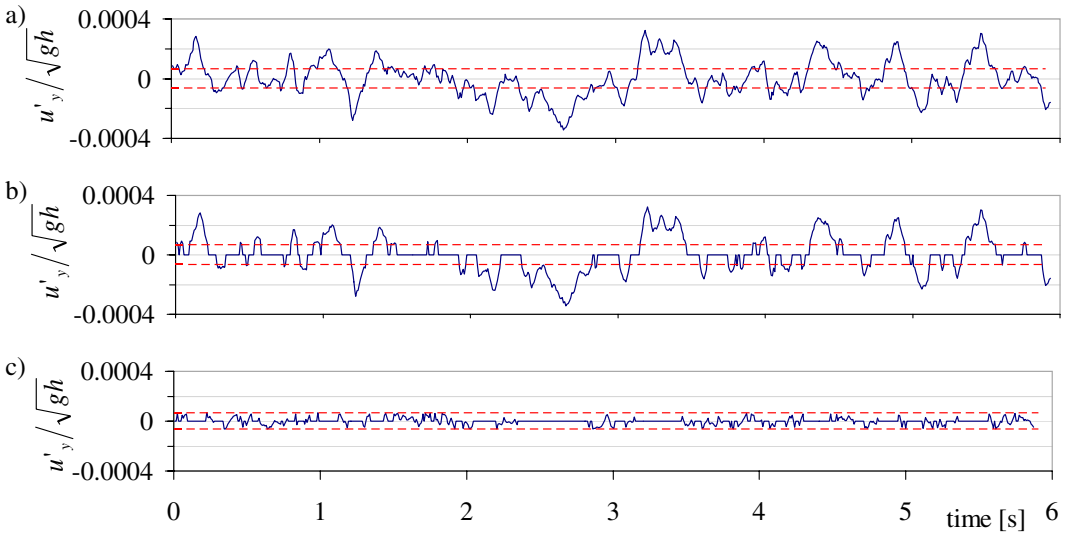

FIG. 5. (Color online) Decomposition of the velocity signal following definition of the intermittence factor ($y/h=0.62$, $\Omega=0.55$): (a) complete signal; (b) collisional part of the signal; (c) frictional part of the signal. Dashed red lines represent the threshold value of the fluctuating component of the velocity given by Eq. (9) used to separate the collisional intervals from the frictional ones.

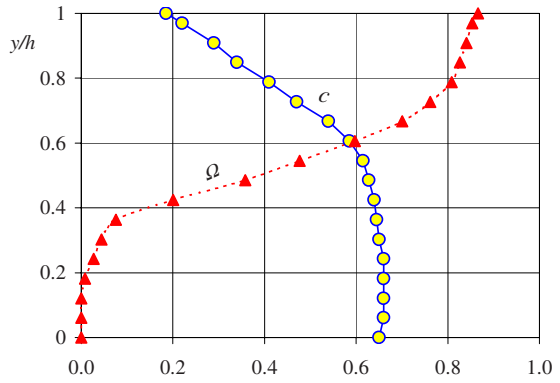

FIG. 6. (Color online) Profiles of particle concentration c and intermittency function Ω; $h=62$ mm, $\alpha=8°$.

ponent of the velocity given by Eq. (11), used to separate the collisional periods from the time intervals dominated by the presence of the frictional regime.

In order to specify the statistics of the intermittent quantities, let us consider first the normal stress consisting of the sum of a collisional stress and a frictional one. We assume that the stress is collisional, σ_c, when the fluctuating component of the velocity exceeds the threshold value; otherwise it is frictional, σ_f. The interparticle's stress, σ_p, is thus decomposed into two contributions

$$\sigma_p = \sigma_f + \sigma_c = (\rho_p - \rho)g \cos \alpha(h-y)\bar{c}. \tag{12}$$

This separation is also significant in terms of the instantaneous values of the stresses in the sense of the continuum mechanics, but in this case the collisional stress does not include the streaming component due to exchange of momentum. We can integrate Eq. (12) in a period T long enough to consider the process as statistically stationary

$$\frac{1}{T}\int_T (\sigma_c + \sigma_f)dt = (\rho_p - \rho)g \cos \alpha(h-y)\frac{1}{T}\int_T \bar{c}dt. \tag{13}$$

We define the following time average quantities: $\langle\sigma_c\rangle = (\int_T \sigma_c dt)/T$, $\langle\sigma_f\rangle = (\int_T \sigma_f dt)/T$, and $\langle\bar{c}\rangle = (\int_T \bar{c}dt)/T$ and, by averaging Eq. (12), we obtain

$$\langle\sigma_c\rangle + \langle\sigma_f\rangle = (\rho_p - \rho)g \cos \alpha(h-y)\langle\bar{c}\rangle. \tag{14}$$

We can now introduce a filter function, f_c, such that $f_c=1$ when the fluctuating component of the velocity exceeds the threshold value and $f_c=0$ otherwise. We can assume that when $f_c=1$, $\sigma_p=\sigma_c$ and when $f_c=0$, we have $\sigma_p=\sigma_f$. We also assume that the time periods when $f_c=1$ and $f_c=0$ are long enough to consider the process as statistically stationary. We define $T_c=\int_T f_c dt$ as the total time during which the stress is collisional. Let us now multiply Eq. (12) by f_c, integrate the products in the period T, and divide the integral by T,

$$\frac{1}{T}\int_T \sigma_p f_c dt = (\rho_p - \rho)g \cos \alpha(h-y)\frac{1}{T}\int_T f_c \bar{c}dt. \tag{15}$$

Because $(\int_T \sigma_p f_c dt)/T = (\int_T \sigma_c dt)/T = \langle\sigma_c\rangle$ from Eq. (15) we obtain

$$\langle\sigma_c\rangle = (\rho_p - \rho)g \cos \alpha(h-y)\frac{1}{T}\int_T f_c \bar{c}dt$$

$$= (\rho_p - \rho)g \cos \alpha(h-y)\frac{T_c}{T}\left(\frac{1}{T_c}\int_{T_c} \bar{c}dt\right). \tag{16}$$

Because $\bar{c}$ is not the local concentration, but is the concentration averaged on the column $h-y$, in Eq. (16) we have assumed that $(\int_{T_c} \bar{c}dt)/T_c = (\int_T \bar{c}dt)/T = \langle\bar{c}\rangle$ and by inverting the order of integration we have

$$\langle\sigma_c\rangle = \Omega\int_y^h (\rho_p - \rho)g \cos \alpha c dy + \langle\sigma_o\rangle, \tag{17}$$

where

$$\Omega = \left(\int_T f_c dt\right)/T = T_c/T \tag{18}$$

is the intermittency function. In Fig. 6 the profile of the intermittency function Ω is reported together with the particle concentration profile. The intermittency function tends to be zero when the concentration tends to particle packing concentration (*frozen concentration*) $c_* \simeq 0.66$. The figure shows that the flow is dominated by the frictional regime in the lower, denser part of the flow; while toward the free surface, where the particles have more possibility to fluctuate, the collisional regime tends to prevail.

In Eq. (17) a normal stress $\langle\sigma_o\rangle$ has been added because, otherwise, one would expect the granular temperature to vanish on the free surface. However, it is easy to argue that the free surface acts as a reflective surface for the temperature when the particle concentration in the layer near to the free surface is sufficiently high. In this situation the particles reaching the free surface, due to inertia, tend to emerge.

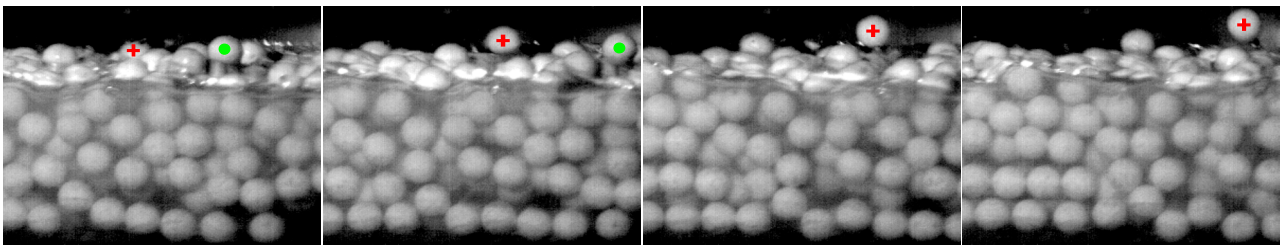

FIG. 7. (Color online) Sequence of images of a granular-liquid uniform flow over a solid bed, acquired through the flume sidewall at a frame rate of 1000 Hz (but presented here at 143 Hz). The particles on top emerge partially (reflective boundary condition) and in some cases jump out of the free surface, as evidenced with the red and green markers (ballistic boundary condition [18]).

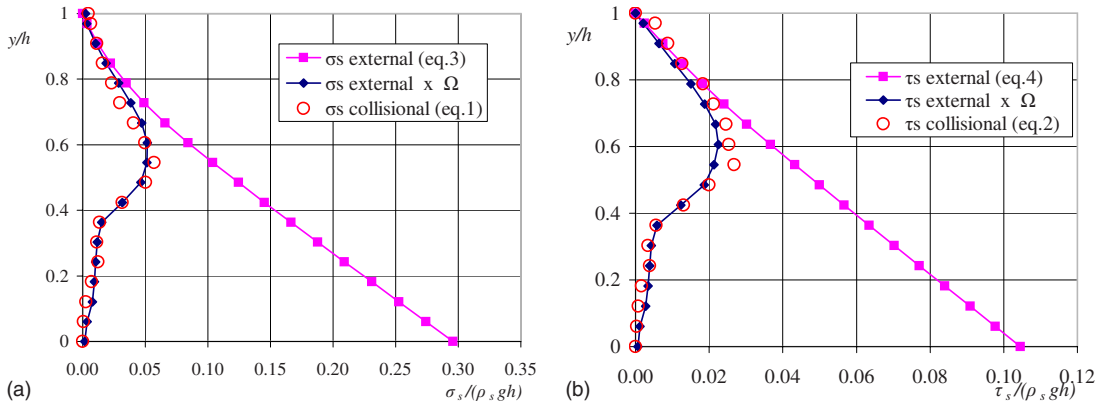

FIG. 8. (Color online) Profiles of external stresses, external stresses reduced according to the intermittency function [right-hand side of Eq. (19)], and the internal ones [Eqs. (1)] calculated on the basis of kinetic theories for the (a) normal and (b) shear stresses, respectively; $h=62$ mm, $\alpha=8°$.

When the emersion starts, in fact, a new force appears (due to the reduction in the buoyancy force), which progressively pushes the particle in the downward direction. This effect, hydrodynamic resistance apart, gives the free surface reflective properties.

In some cases, especially when the slope is high and a fully collisional flow takes place over a solid bed, some particles may emerge completely, make complete jumps out of the water, and plunge back into the water after a ballistic trajectory, as shown in Fig. 7. In this particular case, when integrating the flow equations throughout the flow depth, proper ballistic boundary conditions have to be set on the top of the domain [18]. However, runs presenting a ballistic behavior of top particles have not been considered in the present analysis, owing to the small numbers of these events.

If we operate in the same way with the shear stresses, we obtain

$$\langle \tau_c \rangle = \Omega \int_y^h g[\rho + (\rho_p - \rho)c \sin \alpha dy]. \tag{19}$$

A good agreement between external stresses reduced according to the intermittency function [right-hand side of Eq. (19)] and the internal ones [Eq. (1)], calculated on the basis of kinetic theories, is obtained, as shown in Fig. 8.

Figure 9 reports the distributions of dimensionless particle velocity and dimensionless granular temperature. The asymptotic behavior to zero is confirmed for both the variables when approaching the immobile bed layer.

V. KINETIC-ENERGY BALANCE IN THE COLLISIONAL REGIME

To complete the dynamics of the system, the particle energy balance must be added to the two momentum equations

$$0 = \frac{d}{dy}\left(g_o f_4 \rho_p D \langle \Theta \rangle^{1/2} \frac{d\langle \Theta \rangle}{dy} \right) + \langle \tau_c \rangle \frac{du}{dy} - f_5 (1 - e_p^2) \rho_p \frac{\langle \Theta \rangle^{3/2}}{D}. \tag{20}$$

Equation (20) represents [19] the balance of the particle energy in the collisional regime. The first term of the equation is the diffusion of kinetic energy, the second term is the production of energy due to shear stresses, while the third term represents the energy dissipated during the interparticle collisions. f_4 and f_5 are dimensionless constitutive functions, for which, following Lun *et al.* [13], we have adopted

$$f_4 = \frac{25\sqrt{\pi}}{16\eta_p(41 - 33\eta_p)}\left(1 + \frac{12}{5}\eta_p c g_o\right),$$

$$\left(\frac{1}{g_o} + \frac{12}{5}\eta_p^2(4\eta_p - 3)c\right) + \frac{4}{\sqrt{\pi}}\eta_p c^2 g_o,$$

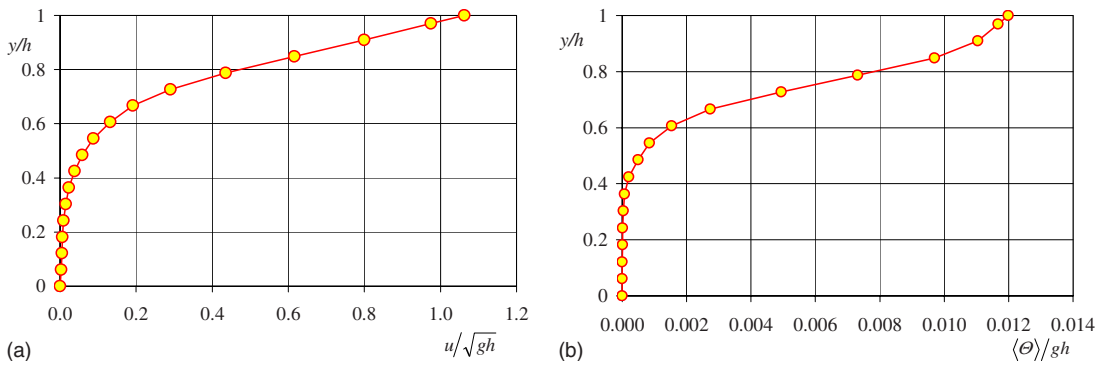

FIG. 9. (Color online) Profiles of dimensionless (a) particle velocity e and (b) granular temperature; $h=62$ mm, $\alpha=8°$.

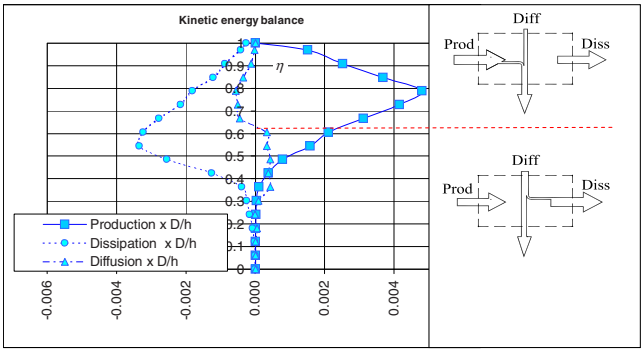

FIG. 10. (Color online) Experimental profiles of dimensionless terms of the kinetic-energy equation balance [Eq. (20)]; $h=62$ mm, $\alpha=8°$.

$$f_5 = \frac{12}{\sqrt{\pi}} c^2 g_o. \tag{21}$$

In the energy balance the effect of a viscous interstitial fluid may be concentrated in the dissipation term, assuming that the presence of the water induces a further reduction in the restitution coefficient [20].

Figure 10 (left) reports the profiles of the three terms forming the kinetic-energy balance. The figure shows that production and dissipation dominate the process, while the diffusion term, even if not negligible, is of minor importance. This term is calculated through a double derivative of the experimental data and it may therefore be affected by substantial experimental errors. The same term, calculated as the difference between the other two, is different from that calculated according to Eq. (20), but with substantially the same trend. As expected, the integral along the depth of this term is close to zero. Its trend is such that the diffusive flux of kinetic energy $d\langle\Theta\rangle/dy$ is always positive; that is, the kinetic energy is diffused toward the bed where it is minor, but it vanishes on the free surface and on the immobile bed, with a maximum in between.

In the layer dominated by collisions, part of the energy produced is dissipated and part is diffused in the downward direction (Fig. 10, right). By contrast, in the layer dominated by frictional contacts the energy locally dissipated by inelastic collisions derives partly from the energy locally produced and partly from the energy coming from above by diffusion.

VI. CONCLUSIONS

The experiments described here have shown that the collisional and frictional regimes are stratified, but with a large layer of interference between the two. The interference layer is dominated by an intermittence between collisional and frictional behaviors.

A special filtering procedure of the signal has made up possible to discriminate between time intervals during which the flow can be considered collisional and governed by the dense gas analogy and time intervals during which the flow has to be considered frictional. The analysis of the signal has also made up possible to define a proper intermittency function, which decreases for increasing values of the particles concentration.

The external stresses reduced according to the intermittency function are in good agreement with the normal and tangential stresses calculated according the kinetic theory, in which the closure functions depend on the inelastic restitution coefficient. The paper also gives the distribution along the flow depth of the different terms that contribute to the particle kinetic-energy equation.

ACKNOWLEDGMENTS

Research carried out with the initial financial support of MIUR/COFINLAB 2001 and within the activities of the European Projects IMPACT (Grant No. EVG1-CT-2001-00037) and IRASMOS (Project No. 018412). The authors are also indebted to the anonymous reviewers for their helpful comments and suggestions.

[1] S. B. Savage, Adv. Appl. Mech. **24**, 289 (1984).
[2] I. Goldhirsch, Annu. Rev. Fluid Mech. **35**, 267 (2003).
[3] S. B. Savage, J. Fluid Mech. **377**, 1 (1998).
[4] G. G. Joseph, R. Zenit, M. L. Hunt, and A. M. Rosenwinkel, J. Fluid Mech. **433**, 329 (2001).
[5] M. Larcher, *Vertical structure of high-concentration liquid-granular flows*, Monographs of the School of Doctoral Studies in Environmental Engineering (Università degli Studi di Trento, Trento, 2004), Vol. 2, p. 144.
[6] A. Armanini, H. Capart, L. Fraccarollo, and M. Larcher, J. Fluid Mech. **532**, 269 (2005).
[7] A. Armanini, L. Fraccarollo, and M. Larcher, Powder Technol. **182**, 218 (2008).
[8] H. Capart, D. L. Young, and Y. Zech, Exp. Fluids **32**, 121 (2002).
[9] B. Spinewine, H. Capart, M. Larcher, and Y. Zech, Exp. Fluids **34**, 227 (2003).
[10] M. Larcher, L. Fraccarollo, A. Armanini, and H. Capart, J. Hydraul. Res. **45**, 59 (2007).
[11] A. T. H. Perng, H. Capart, and H. T. Chou, Granular Matter **8**, 5 (2006).
[12] C. K. K. Lun and S. B. Savage, Acta Mech. **63**, 15 (1986).
[13] C. K. K. Lun, S. B. Savage, D. J. Jeffrey, and N. Chepurniy, J. Fluid Mech. **140**, 223 (1984).
[14] P. Gondret, M. Lance, and L. Petit, Phys. Fluids **14**, 643 (2002).
[15] A. Armanini, L. Fraccarollo, S. Gambarotto, and M. Larcher, *River Flow 2008* (Grafiker, Çesme-Izmir, Turkey, 2008), Vol. 2, p. 1717.
[16] R. H. Davis, J.-M. Serayssol, and E. J. Hinch, J. Fluid Mech. **163**, 479 (1986).
[17] J. O. Hinze, *Turbulence*, McGraw-Hill Series in Mechanical Engineering (McGraw-Hill, New York, 1975).
[18] J. M. Pasini and J. T. Jenkins, Philos. Trans. R. Soc. London, Ser. A **363**, 1625 (2005).
[19] J. T. Jenkins and D. M. Hanes, J. Fluid Mech. **370**, 29 (1998).
[20] R. M. L. Ferreira, Ph.D. thesis, Universidade Técnica de Lisboa, 2005.